FOLDS OF THE NUCLEATION RATE SURFACE ILLUSTRATED WITH THE *n*-PENTANOL-ARGON SYSTEM

M.P. Anisimov, A.G. Nasibulin, S.D. Shandakov, I.I. Shvets, and L.V. Timoshina

Institute of Atmospheric Optics,
Siberian Branch of the Russian Academy of Sciences, Tomsk
Received July 15, 1995

For the first time, we present a topological approach which permits one to develop the theory of atmospheric nucleation on a new axiomatic basis.

INTRODUCTION

Active investigations into application of lasers to atmospheric pollution monitoring started in the second half of 1960s (Ref. 1). Laser made it possible to change in situ investigations for remote ones. This laid a new foundation for operative monitoring of air pollutions and higher reliability of the atmospheric state forecasts. The development of diagnostic technique in this direction led to considerable success.[2] However, as the investigations,[2] showed the existing conceptions of condensation and nucleation of atmospheric vapors must be improved in order to construct a valuable forecast of the atmospheric aerosol over burden. The present-day theories of the phenomena[3] have evident shortcomings although the history of knowledge on metastable states and kinetics of formation of stable phase nuclei is rather long and begins from early 1700s.

"CLASSICAL NUCLEATION THEORY"

As follows from the overview by W. Oswald,[4] in 1724 Fahrenheit published the results of his observations of supercooled states of water deprived of air solved in it. Although these experiments dealt with freezing of liquid water, they were of principle importance in acquiring the knowledge of metastable phase states and their transition into stable states.

Using glacial acetic acid, Lowitz had carried out Fahrenheit's experiments in 1785. Besides, he discovered the supercooling in supersaturated solutions and arrived to a conclusion that supercooling and supersaturation are global properties of the nature. Even first Fahernheit's experiments demonstrated that the presence of the air or particles of dust sharply shortens the lifetime of supersaturated states. Leville (1850) assigned these effects to contact action of some unknown nature.

As it was discovered in the second-half of the 19th century, the air contains microscopic carriers (embryos) of life, i.e., bacteria. By analogy, this lead to the idea that there exist some invisible particles of inorganic matter which are nuclei of a new phase. Lecog de Boisbaudran (1866) experimentally established the fact that spontaneous formation of nuclei may occur only under strong supersaturation; while under weak supersaturation the system may long exist in a nonequilibrium state.

Formation of droplets from vapor was first studied by Coulier (1875) under adiabatic expansion of water vapor in air.[5] One of the modifications of the system made by Wilson for nuclear research was called Wilson chamber. The first theoretical description of the formation of a new phase was performed by J.W. Gibbs in 1878. Gibbs introduced the strict thermodynamic concept of the critical nuclei of a new phase and laid foundation for formal description of nucleation rate (the number of new phase nuclei appearing in a unit volume during a unit time).

Nevertheless only in 1926, Volmer[7] managed to formulate his own theory of a new phase formation and crystal growth. He introduced the concepts of three- and two-dimensional new phase nuclei by connecting their fluctuation formation with the problem on nucleation rate and linear crystallization rate.

Considering the work of nuclei formation as activation energy, Volmer discovered the possibility of describing quantitatively nuclei of a new phase and crystallization. Then the investigator's efforts were directed to the justification of the kinetics of the process. L. Farkas[8] succeeded in this for droplet formation on the basis of the solution of the system of equations proposed by Szilard. Becker and Doring[9] completed the determination of constants in Farkas's theory. They succeeded in generalization of the variety of single molecular acts leading to formation of a new phase.

The most complete form of the nucleation theory was created by Zel'dovich[10] and Frenkel'[11]. This theory was called "classical nucleation theory". In fact no significant changes in the classical nucleation theory occurred since that time. In 1950 H. Reiss[12] generalized the classical theory for nucleation of binary vapor. Recently, the self-consistent form of the classical theory[13] has became very popular. However, the advances in the development of the theory did not lead to a universal nucleation description capable of providing reliable predictions. This suggests an idea of the necessity of seeking new ideas on aerosol formation in a supersaturated vapor.

0235-6880/96/12 997-08 $02.00

CONNECTIONS BETWEEN THE STATE DIAGRAMS AND SURFACES OF VAPOR NUCLEATION RATES

Topological analysis of the nucleation rate surface over the simplest *PT*-diagram with a single triple point, where *P* and *T* are pressure and temperature of the system was proposed in Ref. 14.

Omitting the delay effects of the stationary nucleation rate at rapid formation of vapor supersaturation, let us consider the simplest state diagram with the triple point *t* and the critical point *c*.

Figure 1 shows this diagram in the *PT*-plane. The dashed line *cs* corresponds to the condition of the spinodal decomposition and restricts the domain of vapor supersaturation. In accordance with the theorem from Ref. 15, the nucleation rate at a critical point equals zero. It is rather evident that the spinodal *cs* is a projection of the line of maximum nucleation rates (*lbs*, see Fig. 1) in the space of nucleation rates $J(P, T)$. It is well known that the vapor-liquid equilibrium line does not end at the triple point and has a continuation in the domain of solid (crystalline) states. No supersaturated states are presented by the lines of phase equilibrium and, correspondingly, the nucleation rate here equals zero.[15] It follows that the nucleation rate surface of a liquid spans the lines of zero (*mtc*) and maximum (*lbc*) rates. The temperatures below the triple point correspond to the formation of a metastable liquid (glass formation). The nucleation rate surface of crystals is spanned on the contour 0*nt* what qualitatively correctly reflects the experimental fact that the aerosols with regular crystalline structure appear under relatively weak supersaturation of the vapor. The excess over certain supersaturation threshold leads to glass formation.[16] Even this simplest case demonstrates that the nucleation rate surface is multisheeted (in the present case, it consists of two surfaces). In the general case of a multicomponent system with a set of phase equilibrium lines corresponding to phase transitions of the first kind, there appear corresponding set of nucleation rate surfaces.

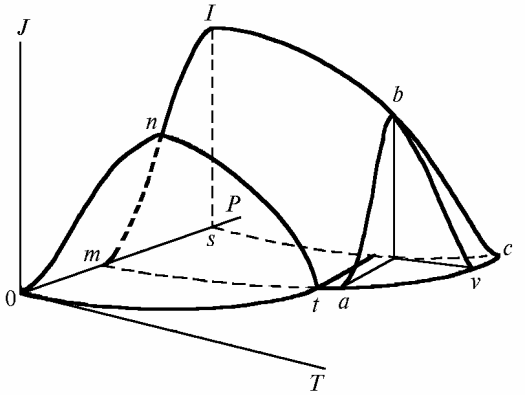

FIG. 1. The surface of nucleation rates over the simplest PT-diagram.

In Ref. 17 we have considered some nucleation rate surfaces for soluble and restrictedly soluble binary systems.

The surface of nucleation rate for a binary system with an eutectic point in the space $J(P, x)$ (x is the composition) is presented in Fig. 2. "inary systems can have several eutectic and peritectic points what, as it is easy to see, leads to further complication of the nucleation rate surface topology. Dissection of surfaces, which are multisheeted in the general case (for instance, under fixed nucleation temperature), must lead to breaks and even jumps at the isotherm of the nucleation rate. This is the result that in no ways follows from the present nucleation theory.

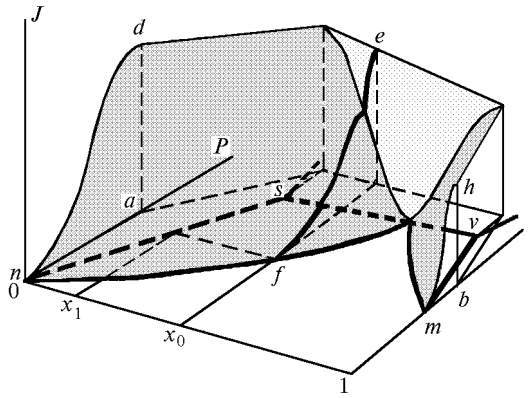

FIG. 2. Nucleation rate surface for a binary system with an eutectic point.

EXPERIMENTAL RESULTS

To verify the results of our qualitative consideration of the nucleation rate surface topology, the *n*-pentanol-argon system was used. The alcohol was chosen in connection with the fact that it, as compared with water, has lower pressure of saturated vapors what considerably helps experimenting. It should be noted that water is formally included in the homologous series of alcohols and the regularities obtained for alcohols can also be valid for the nucleation of water vapor.

The experiment has been performed within the framework of the international experiment on integrating results on the nucleation obtained by different methods at the laboratories leading in the world. All the participants of the integrating used a sample of *n*-pentanol "from the same bottle". It was given by Dr. Reihardt Strey, Max Planck "iophysical Institute (Göttingen, Germany).

The experiment was performed in a flow-line diffusion chamber of our own design.[17] Figure 3 presents the nucleation rate J as a function of chemical activity a of *n*-pentanol vapors in the argon atmosphere. The value of activity is accepted as the ratio of partial pressure of *n*-pentanol to the equilibrium one at the nucleation temperature. The

experiment was performed at 0.20 MPa pressure of the nucleating system and the nucleation temperature was −11.9°C. Experimental values of aerosol the particle concentration (C, cm^{-3}) as a function of temperature of the argon atmosphere saturation (t, °C) with n-pentanol vapor are presented in Table I. The temperature of the wall of the cool thermostat of the aerosol generator was equal to−15.1°C.

TABLE I. Function C(t) for the n-pentanol in argon at a pressure of 0.2 MPa *and temperature of nucleation* (−11.9°C) *and that of the refrigerator* (−15.1°C).

t,°C	log C	t,°C	log C	t,°C	log C	t,°C	log C	t,°C	log C
33.66	0.329	56.26	1.814	79.51	1.881	103.37	4.426	128.55	5.579
34.14	0.359	56.70	1.845	79.96	1.795	103.95	4.443	129.21	5.608
34.44	0.694	57.11	1.470	80.55	2.185	104.48	4.483	130.08	5.600
35.34	0.831	57.48	1.234	80.92	1.613	104.91	4.537	130.60	5.564
36.13	1.117	57.78	1.674	81.39	1.929	105.24	4.554	131.00	5.604
36.61	1.434	58.23	1.833	81.85	2.450	105.67	4.567	131.62	5.614
37.16	1.717	58.86	1.454	82.28	2.063	106.21	4.593	132.16	5.631
37.78	1.895	59.35	1.185	82.70	2.473	106.62	4.642	132.54	5.661
38.30	1.982	59.63	1.701	83.29	2.932	107.01	4.649	133.13	5.662
38.98	2.121	60.20	2.039	83.91	3.177	107.41	4.661	133.79	5.633
39.71	2.222	60.68	1.490	84.51	3.670	107.75	4.696	134.34	5.574
40.32	2.350	61.07	1.189	85.11	3.972	108.10	4.703	135.00	5.555
40.86	2.441	61.42	1.754	85.36	4.199	108.52	4.734	135.57	5.597
41.29	2.549	61.90	2.292	85.86	4.358	108.84	4.753	136.10	5.613
41.79	2.640	62.30	1.965	86.31	4.430	109.25	4.785	136.53	5.586
42.30	2.719	62.61	1.518	86.86	4.030	109.55	4.804	137.13	5.601
42.82	2.732	63.18	1.831	87.32	3.395	109.84	4.835	137.59	5.616
43.42	2.816	63.68	2.215	87.81	3.082	110.44	4.855	138.00	5.631
43.92	3.052	64.19	2.229	88.00	2.877	110.81	4.870	138.81	5.624
44.32	2.989	64.73	1.795	88.40	1.702	111.52	4.886	139.33	5.636
44.83	3.050	65.18	1.765	89.12	2.236	111.86	4.901	139.58	5.612
45.17	3.086	65.60	2.191	89.53	2.547	112.08	4.929	139.82	5.629
45.72	3.025	66.28	2.228	89.88	2.683	112.50	4.944	140.23	5.633
46.16	3.044	66.70	1.959	90.33	2.847	113.20	4.930	140.75	5.665
46.54	3.014	66.95	1.976	90.71	2.863	113.69	4.997	141.13	5.678
46.82	2.732	67.34	2.309	91.18	2.877	113.96	5.030	141.47	5.679
47.35	1.839	67.71	2.242	91.48	2.915	114.25	5.040	142.08	5.610
47.95	2.019	68.34	2.041	91.79	2.920	114.56	5.042	142.62	5.596
48.46	1.850	68.69	2.148	92.21	2.951	114.91	5.083	143.06	5.640
48.69	1.773	69.18	2.448	92.57	2.983	115.41	5.092	143.63	5.649
48.95	1.827	70.00	2.260	92.90	3.006	116.14	5.031	144.04	5.645
49.28	1.852	70.61	2.109	93.48	3.582	116.68	5.126	144.42	5.642
49.63	1.896	71.12	2.362	94.06	3.678	117.31	5.144	144.83	5.619
49.84	1.804	71.73	2.549	94.40	3.659	117.99	5.187	145.19	5.628
50.15	1.553	72.29	2.326	94.80	3.709	118.39	5.219	145.59	5.627
50.42	1.444	72.69	2.254	95.30	3.765	118.97	5.235	145.88	5.638
50.80	1.219	73.24	2.522	95.72	3.782	119.42	5.263	146.19	5.648
51.06	1.247	73.79	2.514	96.14	3.830	119.94	5.289	146.61	5.653
51.27	1.470	74.34	2.318	96.43	3.840	120.56	5.298	147.11	5.646
51.51	1.603	74.68	2.443	96.77	3.833	121.13	5.335	147.60	5.657
51.87	1.743	75.09	2.667	97.43	3.885	121.78	5.354	147.98	5.656
52.25	1.865	75.39	2.430	97.95	3.929	122.38	5.375	148.44	5.657
52.72	1.780	75.87	2.351	98.50	3.981	122.97	5.416	148.94	5.691
53.15	1.424	76.33	2.609	99.13	4.021	123.56	5.443	149.42	5.695
53.39	1.038	76.69	2.533	99.55	4.094	124.31	5.460	–	–
53.64	1.253	77.01	2.317	99.98	4.154	125.04	5.491	–	–
54.15	1.577	77.33	2.404	100.80	4.179	125.60	5.508	–	–
54.64	1.825	77.83	2.499	101.52	4.250	126.30	5.524	–	–
54.96	1.491	78.30	2.097	101.96	4.271	127.00	5.548	–	–
55.33	1.031	78.82	2.066	102.65	4.347	127.55	5.555	–	–
55.83	1.525	79.22	2.356	102.92	4.378	128.08	5.573	–	–

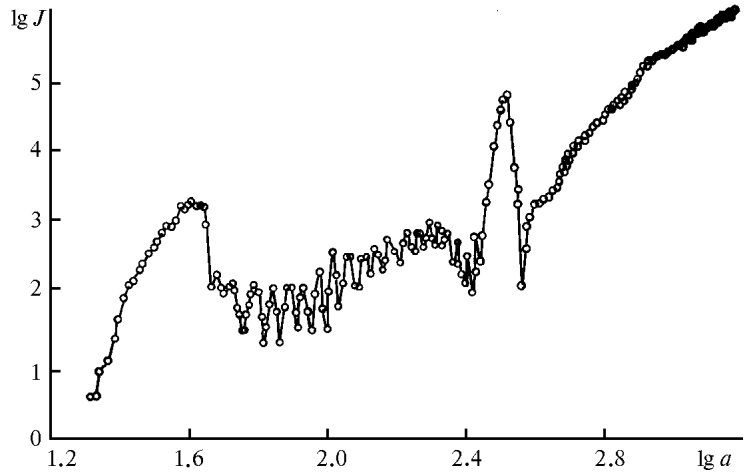

FIG. 3. Nucleation rate (J, $cm^{-3} \cdot s^{-1}$) as a function of n-pentanol vapor activity (a) in the n-pentanol-argon system.

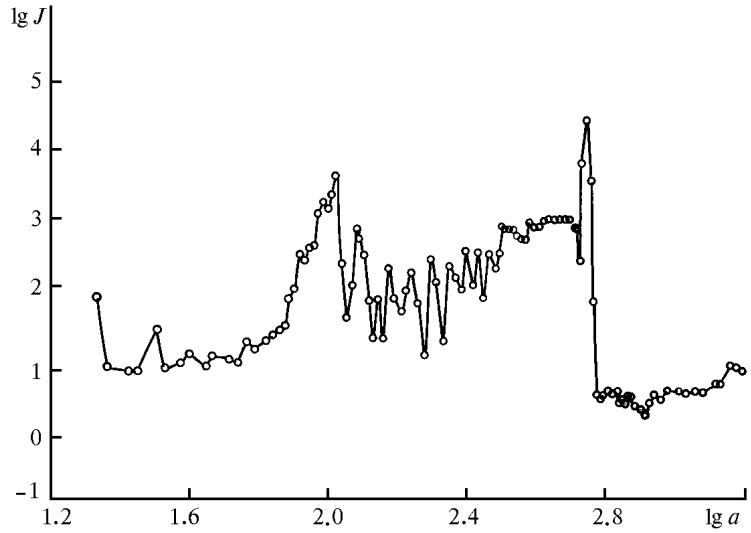

FIG. 4. Nucleation rate (J, $cm^{-3} \cdot s^{-1}$) as a function of n-pentanol vapor activity (a) in the n-pentanol-helium system.

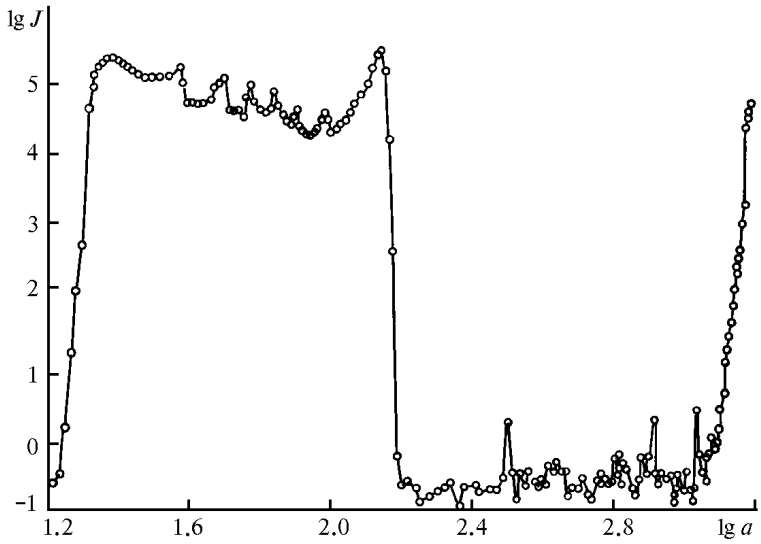

FIG. 5. Nucleation rate (J, $cm^{-3} \cdot s^{-1}$) as a function of n-pentanol vapor activity (a) in the n-pentanol-sulfur hexafluoride system.

In view of the principle novelty of the result obtained on the nucleation of *n*-pentanol vapor in the argon atmosphere, nucleation rates of *n*-pentanol in helium (He) and sulfur hexafluoride (SF_6) were measured. The results are presented in Figs. 4 and 5, respectively. Experimental concentration values as functions of temperature of saturation with *n*-pentanol vapor in the helium and sulfur hexafluoride atmosphere are presented in Tables II and III. The experiments in these gases have been performed at the same pressure of 0.20 MPa. Nucleation temperatures were close to those in argon, namely, −12.5°C in helium, −11,8°C in sulfur hexafluoride what corresponds to temperatures of the refrigerator walls: −14.0°C and −20°C.

The following values were used in calculations for *n*-pentanol: molecular mass $M = 88.150$ g/mole; critical pressure, temperature, density, and volume were equal to: $P_c = 38.97$ bar; $T_c = 588.1$ K; $\rho_c = 0.270$ g/cm^3; $V_c = 326$ cm^3/mole, respectively.[18]

Thermal conductivity of gases is obtained by approximating table values from Ref. 19 using the following polynomial:

$$\chi = T^{1.75}(aP + b) + (P^2c + Pd + e)\ [\mathrm{W\cdot K^{-1}\cdot m^{-1}}] .$$

Approximation constants are presented in Table IV.

Diffusion coefficients in binary gas systems are obtained in accordance with the Fuller-Schettler-Giddings correlation[20] and approximated by the formula

$$D = KT^{1.75}/P ,$$

where the coefficient K for the *n*-pentanol-gas system equals 1.3476E−5 in helium, 3.5830E−6 in argon, and 1.7015E−6 in SF_6.

The pressure of saturated vapor for *n*-pentanol was calculated by the formula

$$P = \exp(A + B/T + C\ln(T))133\ [\mathrm{Pa}] ,$$

where $A = 90.08$; $B = 9788$; $C = -9.90$.[21]

TABLE II. Experimental values of the aerosol concentration (C, cm^{-3}*) as functions of the temperature of helium saturation (t,* °C*) with n-pentanol vapor at the pressure of* 0.2 MPa*. Temperature of the cool thermostat is* −14.0°C*, and the nucleation temperature is* −12.5°C*.*

t,°C	log C	*t*,°C	log C	*t*,°C	log C	*t*,°C	log C	*t*,°C	log C
31.77	1.491	56.39	2.701	72.64	1.556	88.44	2.410	102.79	0.094
32.71	0.500	56.89	2.914	73.44	2.113	88.87	2.371	104.77	0.091
34.86	0.441	57.47	3.217	74.26	1.598	89.18	1.925	105.79	0.050
35.79	0.440	57.91	1.950	74.87	2.084	89.72	3.331	107.56	0.083
37.81	1.031	58.46	1.165	75.63	1.437	90.40	3.923	108.55	0.079
38.44	0.473	59.23	1.637	76.57	2.061	90.89	3.053	110.90	0.188
40.25	0.564	59.72	2.430	77.43	1.842	91.33	1.376	111.67	0.194
41.05	0.696	59.97	2.293	77.81	2.063	91.76	0.050	113.56	0.447
42.79	0.531	60.38	2.042	78.31	2.430	92.03	0.024	114.41	0.409
43.55	0.662	60.68	2.065	78.96	2.395	92.70	0.045	116.10	0.359
45.33	0.608	61.13	1.426	79.64	2.398	93.41	0.110	116.92	0.486
46.09	0.539	61.68	0.884	80.28	2.315	93.62	0.106	118.66	0.460
47.28	0.864	62.10	1.448	80.95	2.252	94.05	0.066	119.60	0.604
47.92	0.750	62.86	0.862	81.45	2.262	94.71	0.091	120.84	0.518
49.31	0.854	63.63	1.887	82.10	2.498	95.14	0.085	121.47	0.578
49.95	0.947	64.28	1.447	82.81	2.411	95.41	0.040	122.75	0.511
50.70	1.023	64.97	1.244	83.29	2.441	95.69	0.062	123.35	0.459
51.38	1.055	65.59	1.558	84.19	2.525	96.11	0.090	124.72	0.599
51.85	1.455	66.34	1.798	84.73	2.578	96.55	0.045	125.70	0.622
52.42	1.583	67.16	1.399	85.04	2.523	96.97	0.028	126.56	0.659
53.10	2.070	68.06	0.627	85.70	2.539	97.49	0.096	127.57	0.716
53.61	1.992	68.84	1.994	86.39	2.541	98.52	0.168	128.50	0.673
54.23	2.162	69.52	1.666	86.70	2.550	99.11	0.255	130.53	0.583
54.75	2.182	70.39	0.840	87.04	2.470	99.74	0.056	131.42	0.600
55.26	2.638	71.21	1.907	87.48	2.527	100.62	0.036	–	–
55.83	2.798	72.00	1.718	87.89	2.527	101.61	0.024	–	–

TABLE III. Function C(t) for n-pentanol nucleation in sulfur hexafluoride at the pressure of 0.2 MPa, *nucleation temperature* −11.8°C. *The temperature of the refrigerator wall is* −20.0°C.

t,°C	log C	t,°C	log C	t,°C	log C	t,°C	log C	t,°C	log C
30.13	−0.301	73.62	5.025	103.75	5.353	151.88	−0.507	188.46	1.330
33.16	−0.310	74.45	5.072	104.43	4.411	152.72	−0.611	189.20	1.533
35.63	−0.410	75.01	5.243	105.31	2.839	153.64	−0.574	189.79	1.776
37.05	−0.507	75.65	5.299	106.22	−0.014	154.64	−0.255	190.31	1.992
39.75	−0.410	76.36	5.357	107.11	−0.435	155.32	−0.522	190.84	2.204
40.91	−0.507	77.13	4.917	107.88	−0.397	155.89	−0.183	191.31	2.326
43.61	−0.539	77.67	4.900	109.49	−0.477	156.47	−0.632	191.64	2.454
44.66	−0.410	78.42	4.904	110.28	−0.675	156.94	−0.341	192.06	2.538
46.97	−0.363	79.00	4.814	112.39	−0.611	157.83	−0.410	192.48	2.903
48.70	−0.213	79.36	4.829	113.74	−0.539	159.43	−0.675	193.33	3.153
49.69	−0.330	79.84	5.072	115.32	−0.477	160.00	−0.808	193.85	4.251
50.80	−0.255	80.36	5.261	116.36	−0.422	161.30	−0.539	193.97	4.248
51.71	−0.141	80.99	5.024	118.06	−0.808	161.80	−0.255	194.54	4.278
52.60	0.519	82.03	4.899	119.04	−0.491	162.91	−0.507	195.17	4.368
53.51	1.556	82.89	4.851	121.43	−0.477	163.65	−0.282	195.67	4.451
54.23	2.403	83.56	4.889	122.21	−0.592	165.39	0.244	196.02	4.507
54.97	3.085	84.03	5.143	124.60	−0.556	165.97	−0.522	196.52	4.557
55.88	4.969	84.76	4.934	125.69	−0.592	166.62	−0.653	196.97	4.725
56.64	5.274	85.58	4.803	127.80	−0.435	167.31	−0.507	197.46	4.754
57.34	5.463	86.01	4.720	128.78	0.348	168.91	−0.574	197.89	4.754
58.09	5.556	86.97	4.692	129.83	−0.341	169.67	−0.539	198.21	4.769
58.80	5.640	87.71	4.767	130.68	−0.750	171.34	−1.000	198.75	4.805
59.49	5.667	88.24	4.862	131.46	−0.363	171.79	−0.723	199.13	4.889
59.91	5.667	88.81	4.619	132.40	−0.556	172.40	−0.556	199.57	4.924
60.47	5.653	89.35	4.580	133.32	−0.341	173.19	−0.750	200.26	4.923
61.18	5.606	89.96	4.537	133.88	−0.912	174.09	−0.491	200.98	4.972
61.81	5.562	90.61	4.508	134.66	−0.491	175.07	−1.176	201.19	4.966
62.31	5.498	91.18	4.552	135.49	−0.556	175.69	−0.750	201.58	5.002
62.79	5.459	91.83	4.609	136.45	−0.477	176.36	−0.954	202.26	5.026
63.25	5.464	92.59	4.724	137.26	−0.539	176.95	−0.750	202.87	5.057
63.84	5.442	93.23	4.825	137.83	−0.282	177.74	0.340	203.18	5.029
64.42	5.389	93.48	4.715	139.23	−0.374	178.53	−0.282	203.90	5.011
64.94	5.426	94.10	4.543	139.94	−0.229	179.52	−0.522	204.98	5.083
65.59	5.401	94.28	4.553	141.30	−0.386	180.66	−0.653	205.79	5.106
66.24	5.398	94.86	4.578	141.82	−0.386	181.40	−0.320	206.46	5.140
67.25	5.409	95.59	4.646	142.89	−0.723	182.09	−0.291	207.11	5.190
67.83	5.418	96.61	4.710	143.54	−0.611	183.08	−0.056	207.25	5.216
69.06	5.529	97.26	4.806	145.28	−0.632	183.80	−0.221	–	–
69.69	5.318	98.29	4.927	145.83	−0.491	184.26	−0.134	–	–
70.41	5.025	99.49	5.045	147.55	−0.723	185.11	0.041	–	–
71.00	5.038	00.54	5.170	148.23	−0.808	185.77	0.344	–	–
71.73	5.009	01.46	5.395	149.88	−0.539	186.43	0.534	–	–
72.49	4.995	02.40	5.599	150.68	−0.435	187.31	0.973	–	–
72.99	4.956	03.19	5.647	151.13	−0.611	187.98	1.150	–	–

TABLE IV.

Gas	*a*	*b*	*c*	*d*	*e*
He	0	9.9323e-2	0	0	2.6025e-6
Ar	−1.4016e-9	3.5861e-7	−2.3030e-7	7.8761e-5	9.7923e-3
SF_6	−1.3454e-8	5.4658e-7	0	4.6048e-4	9.1314e-4

DISCUSSION

As seen from Fig. 3, the nucleation rate as a function of vapor activity has a nontraditional shape. The curve is presented in double logarithmic coordinates, in addition to the smooth and slightly convex rise, it has an abrupt slope and a sharp peak. This behavior well favors our qualitative conclusion about multisheetedness of the nucleation rate surface.

Fluctuations of the nucleation rate are observed between the decrease and peak of the aerosol formation rate. The fluctuations resemble "elousov-Zhabotinskii fluctuations well known in chemistry. Perhaps they are a consequence of a bistability arising with the transfer from one nucleation surface to another. Change of helium for sulfur hexafluoride does not change the behavior. In contrast to SF_6, we failed to detect the second rise in helium in the region of parameter values achievable.

It should be noted that similar manifestations were observed in experiments, but the "prohibition" of the classical nucleation theory led investigators to a search for "experimental errors" or incomplete representations of experimental data.

Our consideration implies nontrivial conclusions. The surfaces of nucleation rate "grow" from state diagrams. However, it is well known that scaling for state diagrams is not yet developed in the general form. This means that the hope to develop a universal nucleation theory based on the molecular kinetic position is groundless as long as there is no strict molecular kinetic justification of the phase diagrams. Thus far, only empirical determinations of the phase diagrams then followed by a construction of the rate surface using experimentally determined values of the nucleation rate are promising. Creation of semiempiric computational approximations is possible for some classes of systems. In the final analysis, the hope to construct a universal nucleation theory is lost for a long time. However, not a simple but quite a comprehensive topological way of developing the nucleation theory is opened.

CONCLUSIONS

At present, empirical determination of the state diagrams of corresponding vapor-gas systems are necessary to describe atmospheric nucleation. Temperature-pressure diagrams for water and temperature-composition diagrams for some binary systems with water already exist. "ut pressure-composition diagrams for binary systems, which are necessary for the topological approach, must be improved. Laboratory experiments whose number can be reduced owing to the new approach by orders of magnitude will make it possible to normalize the nucleation rate scales. At present, this way seems to be true for a successful improvement of our knowledge of homogeneous and heterogeneous nucleation in the atmosphere.

ACKNOWLEDGMENTS

The authors would like to acknowledge Russian Foundation of Fundamental Research for the Grant No. 94−03−09947 and Dr. Reinhardt Strey for giving a sample of *n*-pentanol.

REFERENCES

1. V.E. Zuev, M.V. Kabanov, and ".A. Savel'jev, Appl. Opt. **8**, No. 1, 137−141 (1969).
2. V.E. Zuev and G.M. Krekov, *Optical Models of the Atmosphere* (Nauka, Novosibirsk, 1988), 250 pp.
3. A.G. Amelin, *Theoretical Foundations of Mist Formation at Vapor Condensation* (Khimiya, Moscow, 1972), 304 pp.
4. W. Ostwald, *Lehrbuch der Allgemeinen Chemie* (Leipzig, 1896−1902), 230 pp.
5. W. Aitken, Trans. Soc. Edinb. **30**, 337−345 (1880).
6. J.W. Gibbs, Amer. J. Sci. and Arts **XVI**, 454−457 (1878).
7. M. Volmer and A. Weber, Z. Physik. Chem. **Bd119**, 277−282 (1926).
8. L. Farkas, Z. Physik. Chem. **125**, 236−242 (1927).
9. R. "ecker and W. Doring, Ann. Physik. **7**, 13−17 (1921).
10. Ya." . Zel'dovich, Zh. Eks. Teor. Fiz. **12**, 525−538 (1942).
11. Ya.I. Frenkel', *Kinetic Theory of Liquids* (Nauka, Leningrad, 1975), 592 pp.
12. H. Reiss, J. Chem. Phys. **18**, 840−848 (1950).
13. G. Wilemski, J. Chem. Phys. **103(3)** 1119−1126 (1995).
14. M.P. Anisimov, J. Aerosol Sci. **21**, Suppl. 1, 23−26 (1990).
15. M.P. Anisimov, in: *AEROSOLS Their Generation, Behaviour and Applications Norwich, the University of East Anglia,* 1995, pp. 201−206.
16. M.P. Anisimov, in: *Nucleation and Atmospheric Aerosols*, K. Fukuta and P.E. Wagner, eds. (Pergamon Press, Virginia, 1992), pp. 451−455.

17. M.P. Anisimov, A.G. Nasibulin, S.D. Shandakov, and N.I. Gordienok, Atmos. Oceanic Opt. **9**, No. 6, 555–560 (1996).
18. M. Gude and A.S. Teja, J. Chem. Eng. Data **40**, 1025–1036 (1995).
19. N.V. Vargaftik, L.P. Filippov, A.A. Tarmazinov, and E.E. Totskii, *Handbook on Thermal Conductivity of Liquids and Gases* (Energoizdat, Moscow, 1990), 708 pp.
20. R.C. Reid, J.M. Prausnitz, and T.K. Sherwood, *The Properties of Gases and Liquids* (McGraw-Hill "ook Company, New York etc., 1977).
21. R. Strey and T. Schmeling, "er. "unsen-Ges. Phys. Chem. **87**, 323 (1983).